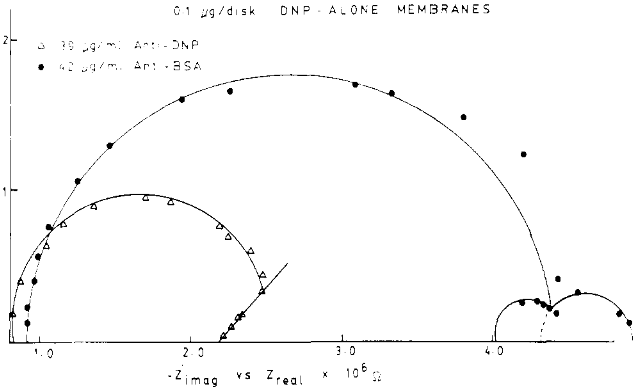

Figure 20. Comparison of impedance responses to anti-DNP, △, and to anti-BSA, ○, at a membrane containing 0.1 μg/disk DNP alone.

represents the magnitude of charge carriers within the interior of the membrane, is essentially the same when exposed to marker ion and antibody. This would not be expected if the binding of antibody to antigen was significantly removing DNP (antigen carrier) from within the interior of the membrane.

This notion is also supported in a second experiment where a membrane containing a 1.0 μg/disk concentration of DNP alone was exposed to analyte solution containing 109 μg of anti-DNP/mL for 2.5 h with stirring. The ac impedance plot was obtained before and after conditioning in antibody and, in each case, the solutions contained 10^{-3} M KCl in buffer/electrolyte. Though the membrane bulk resistance component increased from 10.4 to 13.2 MΩ, the bulk capacitive component still remained essentially the same, i.e., from 1.02×10^{-10} to 1.0×10^{-10} F.

Finally, the ac impedance plot for a 0.1 μg/disk DNP-alone membrane exposed to comparable concentrations of anti-DNP and anti-BSA are shown in Figure 20. Clearly the overlapping semicircles obtained at low frequencies for the anti-BSA analyte are different than the behavior observed for the selective DNP antibody. This indicates that the interfacial features cognizant in a selective protein adsorption process are characteristically distinct from the nonselective adsorption-type interaction depicted for anti-BSA. This would be expected on the basis of an additional binding affinity for the interaction of a specific antibody with its antigen.

In summary, both the galvanostatic and ac impedance measurements support a model for immunosensors in which the observed potentiometric response can be related to modulation of exchange currents resulting from the selective immunoreaction between specific antibody and antigenic ionophore or antigen conjugated with ionophore. Consequently, very simple immunosensors can be constructed for those cases where the antigen has some ionophoric function.

Acknowledgment. We gratefully acknowledge the support of National Institutes of Health Grant GM-25308.

High-Energy Resolution X-ray Photoelectron Spectroscopy Studies of Tetracyanoquinodimethane Charge-Transfer Complexes with Copper, Nickel, and Lithium

John M. Lindquist† and John C. Hemminger*

Institute for Surface and Interface Science and Department of Chemistry, University of California, Irvine, California 92717

Received July 28, 1988

X-ray photoelectron spectra are presented for LiTCNQ, $Ni(TCNQ)_2{\cdot}3H_2O$, CuTCNQ, and $Cu(TCNQ)_2$ (TCNQ = tetracyanoquinodimethane). The $Cu(TCNQ)_2$ compound is shown to be of a mixed valence character: $Cu^+(TCNQ^-)(TCNQ^0)$. The TCNQ component in all the other complexes is well described as $TCNQ^-$. The detailed shape of the shakeup intensity observed in both C 1s and N 1s spectra is discussed in comparison with the trend of electrical conductivity in these compounds. We suggest that the valence orbital involved in the strong XPS shakeup intensity for $TCNQ^0$ is involved in the conductivity in the charge-transfer complexes.

Introduction

For more than 2 decades the strong electron-acceptor tetracyanoquinodimethane (TCNQ) has been the subject of many studies. Throughout this period a number of intriguing applications have been proposed that make use of this unique molecule and also the charge-transfer complexes it forms with many organic and metal electron-donor species.[1,2] These applications include use of the charge-transfer complexes in optical recording disks,[1] molecular electronic devices,[1] and corrosion inhibition.[2] These applications as well as a fundamental concern with the charge-transfer process have resulted in much interest in the mechanism of TCNQ compound formation.

With regard to charge transfer we are interested in the nature of the TCNQ molecular orbitals involved in this process and how their character changes as a function of charge shifting upon complex formation. Lin et al.[3] have

---

† Present address: Aerojet ElectroSystems Co., MS 170-8244, PO Box 296, Azusa, CA 91702.

(1) Potember, R. S.; Hoffman, R. C.; Hu, H. S.; Cocchiaro, J. E.; Viands, C. A.; Poehler, T. O. *Polym. J.* **1987**, *19*, 147.

(2) Lindquist, J. M.; Giergiel, J.; Hemminger, J. C., data to be published from our laboratory indicates that stable high-temperature TCNQ films can be produced on transition-metal surfaces.

(3) Lin, S. F.; Spicer, W. E.; Schechtman, B. H. *Phys. Rev. B* **1975**, *12*, 4184.

0897-4756/89/2801-0072$01.50/0 © 1989 American Chemical Society

proposed that the transferred charge is localized on a molecular scale and that TCNQ will exist in either a −1 or neutral charge state. This implies the TCNQ orbitals do not overlap appreciably with the donor molecular orbitals after compound formation and thus the interaction between them is largely electrostatic. Evidence for this has been shown in both core and valence level photoemission spectra of tetrathiofulvalinium TCNQ (TTF-TCNQ).[4-6] The localization of this charge within the TCNQ molecule itself however has not been addressed experimentally. A theoretical study of $TCNQ^0$, $TCNQ^-$, and $TCNQ^{2-}$ by Jonkman et al.[7] indicates that transferred charge is localized on the methylene type carbons in $TCNQ^-$. To the best of our knowledge no experimental evidence for this charge localization has been presented.

The unusually high electrical conductivity of many TCNQ charge-transfer complexes generated much interest in the subject of organic metals in the mid- to late-1970s. An excellent review of this subject by Torrance[8] brought together much of what was known concerning electrical conductivity and these types of compounds. An important conclusion from that report pointed toward incomplete charge transfer as a necessary condition for these compounds to exhibit high electrical conductivity. The term incomplete here is not meant to imply a partial electron transfer or sharing of electron density between TCNQ and the donor species but a complete electron transfer to only some TCNQ moieties. The presence of two N 1s features in the X-ray photoelectron spectrum of TTF-TCNQ gives direct evidence for this effect.[4,5] This has also been proposed as an explanation of the relatively high electrical conductivity of $Cu(TCNQ)_2$ by Melby et al.[9]

Recent work in our laboratory indicates thin films of TCNQ on a single-crystal Ni surface are present to temperatures in excess of 500 °C.[2] The high-temperature stability of this surface species may lead to the use of TCNQ as an anticorrosive compound. We are interested in the identity of this stable surface species and, in general, the mechanism of TCNQ interaction with metal surfaces. This topic has been explored previously by Lin et al.[3] for the initial stages of interaction between Cs and TCNQ and by Erley and Ibach studying TCNQ grown on the Cu (111) surface.[10] The dynamics of compound formation may be significantly different for the two donors. Consistent with the above proposition, only neutral and −1 charged TCNQ species are present after compound formation at low Cs exposure to TCNQ.[3] Contrary to this behavior Erley et al.[10] propose the existence of a multiply charged TCNQ at submonolayer coverage on Cu (111). Further exposure of TCNQ to this surface is proposed to form singularly charged and neutral TCNQ in the second and third or greater layers, respectively. The effects of TCNQ on the donor (surface atom) have not been discussed in detail. This is of interest in surface corrosion inhibition and may be meaningful in relation to the differences of interaction of TCNQ with Cs and Cu.

In this report we utilize X-ray photoelectron spectroscopy (XPS) to study charge transfer in a number of metal–TCNQ complexes. XP spectra of these compounds are compared with those of neutral TCNQ to probe the effects of charge transfer on both the core and valence levels of TCNQ. These XP spectra were taken at high-energy resolution which allows separation of the C 1s features in both $TCNQ^0$ and the charge-transfer species. Binding energy shifts of these features vary in magnitude upon complexation and are useful as probes of the localization of transferred charge in these compounds. Spectra are presented for complexes with both high and low electrical conductivity. These spectra indicate the presence of both neutral and singly charged TCNQ in $Cu(TCNQ)_2$. The effect of charge transfer on the metal core level spectra is also discussed. XP spectra from the compounds in this study are compared with those of the pure metal and also other metal cyanide compounds. The spectra here will also be used for comparison with those of TCNQ thin films on metal surfaces and may be helpful in determining the extent of interaction of TCNQ with a surface and the presence or absence of multiply charged TCNQ species.

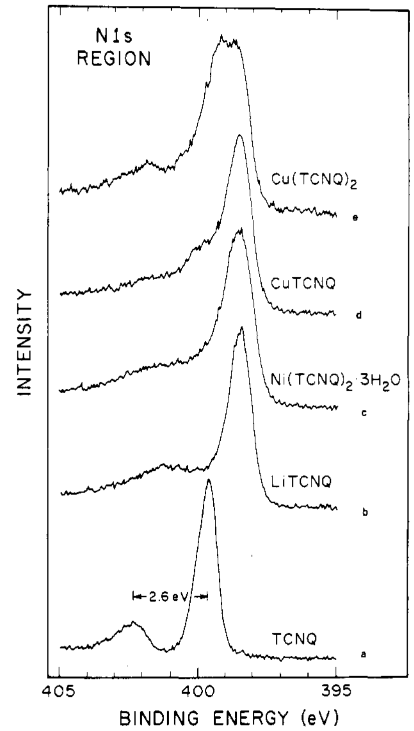

Figure 1. N 1s region high-resolution X-ray photoelectron spectra of $TCNQ^0$ (a) and charge-transfer compounds found with lithium (b), nickel (c), and copper (d, e).

Experimental Section

Experiments were carried out with a VG ESCALAB Mk.II surface analysis system. The electron-energy analyzer was calibrated to the Ag $3d_{5/2}$ line at 368.2 eV. C 1s and N 1s XP spectra were collected by using Al Kα excitation in conjunction with a quartz crystal monochromator, with the electron-energy analyzer set for a constant analyzer energy of 10 eV. The experimental contribution to the peak energy width is approximately 0.60 eV in this configuration.

All metal charge-transfer salts were prepared by the method of Melby et al.[9] All compounds formed as powders and showed no evidence of large crystal growth. In the case of CuTCNQ the compound stoichoimetry was confirmed by elemental analysis.[11] Samples were prepared for analysis by pressing the powder into a Ag-painted sample-holding stub. These samples were checked for contamination from undesirable reagent materials by XPS

---

(4) Grobman, W. D.; Pollack, R. A.; Eastman, D. E.; Maas, E. T., Jr.; Scott, B. A. *Phys. Rev. Lett.* **1974**, *32*, 534.

(5) Grobman, W. D.; Silverman, B. D. *Solid State Commun.* **1976**, *19*, 319.

(6) Ikemoto, I.; Sugano, T.; Kuroda, H. *Chem. Phys. Lett.* **1977**, *49*, 45.

(7) Jonkman, H. T.; van der Velde, G. A.; Nieuwpoort, W. C. *Chem. Phys. Lett.* **1974**, *25*, 62.

(8) Torrance, J. B. *Acc. Chem. Res.* **1979**, *12*, 79.

(9) Melby, L. R.; Herther, R. J.; Mahler, W.; Benson, R. E.; Mochel, W. E. *J. Am. Chem. Soc.* **1962**, *84*, 3374.

(10) Erley, W.; Ibach, H. *Surf. Sci.* **1986**, *178*, 565.

(11) Theoretical %: C, 53.9; H, 1.5; N, 20.9; Cu, 23.7. Experimental %: C, 52.62; H, 1.35; N, 20.89; Cu, 23.98.

Table I. C 1s and N 1s Binding Energies for TCNQ^0 and TCNQ Charge-Transfer Complexes

sample	C 1s binding energy, eV	N 1s binding energy, eV
TCNQ^0	286.6, 285.3, 289.2 (satellite)	399.5, 402.1 (satellite)
LiTCNQ	286.1, 285.0, 284.3, 288.7 (satellite)	398.6, 401.2 (satellite)
Ni(TCNQ)$_2$·3(H$_2$O)	285.9, 285.1, 284.3, 288.5 (satellite)	398.6, ~401. (satellite)
CuTCNQ	285.9, 285.0, 284.3	398.6, ~400. (satellite)
Cu(TCNQ)$_2$	286.6, 285.4, 289.2 (satellite)	398.8, 399.3, 401.9 (satellite)

and rinsed with the solvent for that particular reaction until spectra showed predominantly the presence of only TCNQ and the particular metal donor species.

Spectra from the parent molecule, i.e., pure TCNQ, were obtained from three types of samples: (1) unpurified powder as delivered from the manufacturer, (2) crystals (ca. 2 mm × 2 mm) obtained from recrystallization of TCNQ in CH_3CN, and (3) a thin film deposted on a sample stub by placing a drop of TCNQ-saturated CH_3CN on the stub and allowing the solvent to evaporate. Spectra from all samples were identical, indicating that purification and sample thickness had no effect on C 1s and N 1s binding energies.

Results

N 1s Region. N 1s spectra for TCNQ^0 and the prepared charge-transfer salts are shown in Figure 1. The spectrum for TCNQ^0, shown in the bottom of Figure 1, has been previously discussed in detail.[2] The TCNQ^0 spectrum consists of a relatively intense peak at 399.5 eV with a smaller peak at 402.1 eV. This small peak has been ascribed to an intramolecular excitation in the final-state photoion (commonly referred to as shakeup). The high-energy resolution of this spectrum allows us to attain accurate binding energies for these two features that will become important in comparison with spectra for the TCNQ charge-transfer salts.

The remaining spectra in Figure 1 cover the N 1s region photoelectron spectrum for the Cu, Li, and Ni TCNQ charge-transfer salts. The spectra for LiTCNQ, Ni(TCNQ)·3H$_2$O, and CuTCNQ appear qualitatively similar. The main peak in these spectra is shifted ca. 1 eV to lower binding energy relative to the N 1s feature for TCNQ^0. The spectrum for Cu(TCNQ)$_2$ is significantly different from the other three charge-transfer compound spectra. The main feature in the Cu(TCNQ)$_2$ spectrum is a doublet, indicating the presence of at least two chemical environments in the region of the TCNQ cyano groups. The shakeup feature discussed for the TCNQ^0 N 1s spectrum appears in varying intensity and possibly three different binding energies in Figure 1b–e. As shown in Figure 1b the shakeup feature in the LiTCNQ N 1s spectrum appears 2.6 eV to higher binding energy than the main peak, unchanged from the binding-energy difference of the same features in the TCNQ^0 spectrum of Figure 1a. The Ni(TCNQ)$_2$·3H$_2$O N 1s spectrum is quite similar to that for LiTCNQ with a somewhat broader and thus less prominent shakeup feature. The main N 1s feature in Figure 1d is at similar binding energy to those in Figure 1b,c, but the shakeup feature appears at 399.8 eV, a difference of only 1.2 eV from the main peak. The shakeup feature in the N 1s spectrum for Cu(TCNQ)$_2$ has a binding energy of 402.1 eV, coincident in energy with the shakeup feature for TCNQ^0 in Figure 1a. Binding energies for each feature in Figure 1 are listed in Table I.

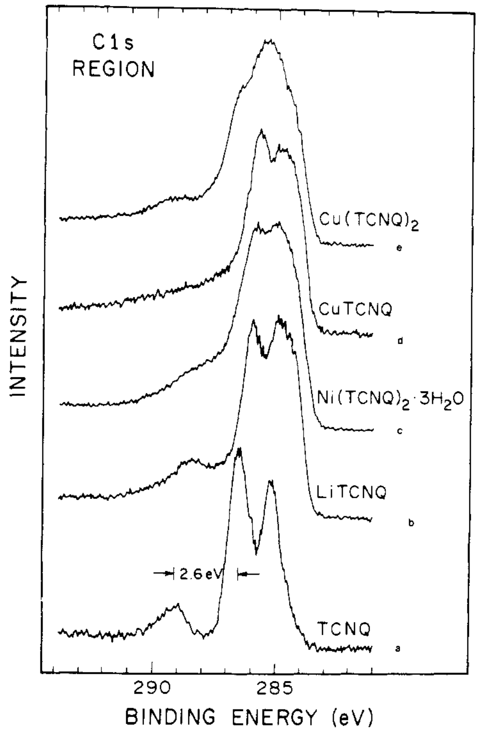

Figure 2. C 1s region high-resolution X-ray photoelectron spectra of TCNQ^0 (a) and its compound formed with lithium (b), nickel (c), and copper (d, e).

C 1s Region. Spectra over the C 1s region for TCNQ^0 and the charge-transfer salts prepared for this study are shown in Figure 2. Binding energies of features in each spectrum are listed in Table I. The XP spectrum of solid TCNQ (Figure 2a) has been presented previously and discussed in detail.[12] The 285.3-eV peak in the solid TCNQ spectrum has been associated with emission from ring carbons. The 286.6-eV peak is due to C 1s emission from the cyano and methylene type carbons. The feature at 289.2 eV is a shakeup satellite that occurs due to an electronic excitation in the molecule upon core-hole creation associated with the cyano and methylene carbons. As discussed in ref 12, core-hole creation on the ring carbons does not lead to a localized shakeup feature. The high-energy resolution of these data compared with that previously presented for TCNQ^0 (ref 13) allows precise determination of the binding energy of this shakeup feature and also its relative intensity, as there is minimal overlap from other features in the spectrum. It is shown in Figure 2a that the 289.2-eV shakeup peak has approximately 20% the intensity of the 286.6-eV peak. It is also apparent that the widths of the two main peaks in Figure 2a are approximately equal. The remainder of the spectra in Figure 2 correspond to the four charge-transfer complexes prepared for this study.

We immediately note a number of differences between the C 1s spectra of the salts and that for pure TCNQ^0. In all spectra for the charge-transfer compounds the separation of the two main peaks is significantly reduced compared with the parent compound. For example, in LiTCNQ the separation of the two main peaks is 1.0 eV, whereas in TCNQ^0 the separation is 1.3 eV. As was observed for the N 1s spectra of TCNQ^0 and the charge-transfer compounds, the C 1s spectra for LiTCNQ, Ni(TCNQ)·3H$_2$O, and CuTCNQ all appear qualitatively similar. The C 1s spectrum for Cu(TCNQ)$_2$ is much different from C 1s spectra of the other salts. The Cu-

---

(12) Lindquist, J. M.; Hemminger, J. C. *J. Phys. Chem.* **1988**, *92*, 1394.

(13) Ikemoto, I.; Thomas, J. M.; Kuroda, H. *Faraday Discuss. Chem. Soc.* 1972, *54*, 208.

Table II. Metal Binding Energies and Auger Parameters of TCNQ Charge-Transfer Complexes

	binding energies, eV				Auger parameter
compd	1s	$2p_{3/2}$	$3p_{3/2}$	3s	
CuTCNQ		931.7	74.8	121.7	1847.9
$Cu(TCNQ)_2$		932.1	75.2	122.2	1847.6
Cu metal[a]		932.7	75.1	122.5	1851.2
Cu metal[b]		932.7	75.1		
Cu metal[c,d]		932.4			1851.0
CuCN[c]		932.9			1847.5
CuCN[d]					1847.5
$Ni(TCNQ)_2 \cdot 3(H_2O)$		857.4	69.2	114.3	1698.4
Ni metal[a]		852.7	66.4	110.9	1698.8
Ni metal[c]		852.3			1698.5
LiTCNQ	55.6				
LiF[e]	55.5				

[a] This work. [b] Seah, M. P. *J. Vac. Sci. Technol.* **1985**, *3*, 1330. [c] Wagner, C. D.; Gale, L. H.; Raymond, R. H. *Anal. Chem.* **1979**, *51*, 466. [d] Klean; Proctor; Hercules; Block, *Anal. Chem.* **1983**, *55*, 2055. [e] Wagner, C. D.; Riggs, W. M.; Davis, L. E.; Moulder, J. F. *Handbook of X-Ray Photoelectron Spectroscopy*; Muilenderg, G. E., Ed.; Perkin Elmer Corp., Physical Electronics Division, 1979.

Table III

sample	room-temp conductivity, $(\Omega\ cm)^{-1}$
TCNQ	1×10^{-11}
LiTCNQ	5×10^{-6}
Ni $(TCNQ)_2 \cdot 3H_2O$	1×10^{-4}
Cu(TCNQ)	5×10^{-3}
$Cu(TCNQ)_2$	5×10^{-3}

[a] From: Afify, H. H.; Abdel-Kerim, F. M.; Aly, H. F.; Shabaka, A. A. *Z. Naturforsch.* **1978**, *33*, 344.

$(TCNQ)_2$ spectrum in Figure 2e appears as a complex feature at 284–286 eV with a small but obvious shakeup feature at 289.2 eV, coincident in energy with the shakeup peak of $TCNQ^0$ in Figure 2a. As noted for spectra of the salts in the N 1s region, the shakeup features in the C 1s region spectra appear with varying intensities. The shakeup peak in Figure 2b appears 2.6 eV to greater binding energy than the higher C 1s main feature, mimicking the position of the LiTCNQ shakeup feature in Figure 1b. A shakeup peak is also present in Figure 2c for $Ni(TCNQ)_2 \cdot 3H_2O$ but is broader than in the LiTCNQ spectrum, again similar to the N 1s spectrum. Also, the C 1s spectrum of the CuTCNQ compound shows no localized shakeup feature.

Metal Core Level Regions. Spectra over the metal core level regions for the TCNQ complexes allow analysis of the effect of charge donation on the metal atom. Table III lists measured metal core level binding energies for the charge-transfer complexes prepared for this study along with literature values for a variety of other metal salts. Core level spectra for the charge-transfer compounds with Cu as the donor atom are shown in Figure 3 along with the spectrum for metallic Cu. The Cu $2p_{3/2}$ peaks for CuTCNQ and $Cu(TCNQ)_2$ appear at *lower* binding energies than that for metallic Cu, also shown in Figure 3, in spite of the metal oxidation which commonly yields an increase in measured binding energies. This effect is also noted in the Cu 3s binding energies listed in Table II. Table II also lists the modified Auger parameter for Cu metal, the Cu–TCNQ compounds, and CuCN. Not unexpectedly, these values show that the modified Auger parameter for the Cu–TCNQ compounds are quite similar to that of CuCN but quite different from that for Cu metal. Figure 3, which covers the entire Cu 2p region, also shows lack of intensity in the region between 940 and 945 eV, where shakeup intensity from Cu(II) would appear.

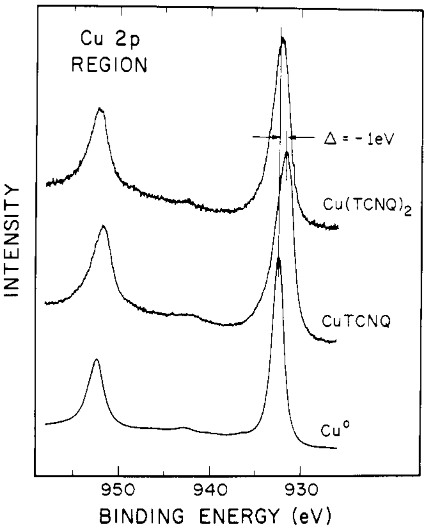

Figure 3. Cu 2p region X-ray photoelectron spectra of Cu^0 and the two Cu–TCNQ compounds studied in this work. Note the shift to lower binding energy of the Cu $2p_{3/2}$ peaks for both Cu–TCNQ compounds relative to that for Cu^0.

Binding energy values obtained for $Ni(TCNQ)_2 \cdot 3H_2O$ core levels listed in Table I are all much greater than for Ni metal. The Ni $2p_{3/2}$ binding energy appears more than 4.5 eV to higher binding energy in $Ni(TCNQ)_2 \cdot 3H_2O$ than the same peak in Ni metal. Contrary to this behavior, the modified Auger parameter for $Ni(TCNQ)_2 \cdot 3H_2O$ is within 0.5 eV of that for Ni metal.

The Li 1s peak is centered at 55.6 eV in LiTCNQ. This value is quite similar to the Li 1s binding energy in LiF at 55.5 eV as shown in Table II.

Discussion

N 1s Region. Spectra for the TCNQ salts all show a shift of 1 eV to lower binding energy for the main N 1s feature. This is consistent with a transfer of electron density from the metal atom to regions of the TCNQ molecule localized near the cyano groups. The N 1s main peak binding energy of 398.6 eV is consistent with that observed by Grobman et al.[4,5] for KTCNQ. It is thus apparent that the TCNQ species in the charge-transfer complexes prepared for this study are in similar oxidation state as the TCNQ species in KTCNQ. In addition, Lin et al.[3] have shown that the TCNQ molecule in solids exists in either the neutral or −1 charge state. From this we conclude that the N 1s binding energy in $TCNQ^-$ is 398.6 eV. Lin et al.[3] also point out that excess charge on $TCNQ^-$ is localized on a molecular scale. The above data indicate some portion of this charge is present at the ends of the molecule, i.e., the cyano ends of the molecule. This is consistent with an earlier report from this laboratory that shows the lowest unoccupied molecular orbital (LUMO) of $TCNQ^0$ has some spatial extent near the cyano groups.[12]

The most intense N 1s feature in $Cu(TCNQ)_2$ appears as a doublet, significantly different from the other charge-transfer salts. One feature appears at nominally 399.2 eV and the other at ca. 398.8 eV, which is quite close to the binding energy for $TCNQ^-$. In the initial work on the preparation and characterization of these compounds by Melby et al.[9] it was postulated that $Cu(TCNQ)_2$ may be composed of one neutral and one singly charged TCNQ species, with Cu in a +1 oxidation state, i.e., $Cu(TCNQ^0)(TCNQ^-)$, a mixed-valence molecular configuration. This is opposed to two TCNQ anions and a Cu(II) cation, $Cu^{II}(TCNQ^-)_2$. However, prior to the work presented here, no definitive experimental evidence existed to

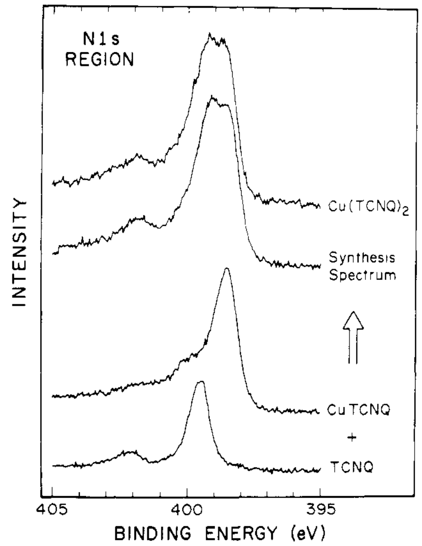

Figure 4. N 1s region X-ray photoelectron spectra of $TCNQ^0$ and CuTCNQ indicating their sum (synthesis spectrum) is quite similar to the N 1s spectrum of $Cu(TCNQ)_2$.

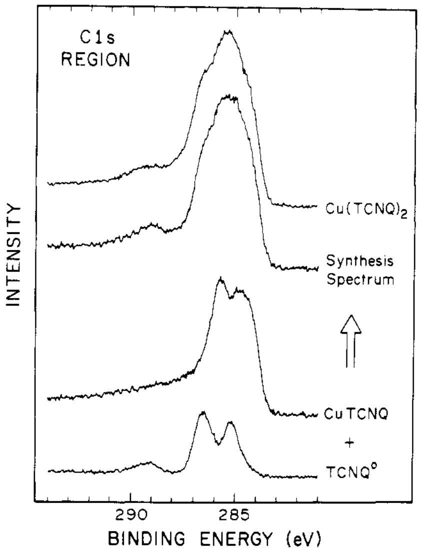

Figure 5. C 1s region X-ray photoelectron spectra of $TCNQ^0$ and CuTCNQ indicating their sum (synthesis spectrum) is quite similar to the N 1s spectrum of $Cu(TCNQ)_2$.

substantiate this view. The presence of two main features in the N 1s spectrum of $Cu(TCNQ)_2$ shown in Figure 1e indicates that $Cu(TCNQ)_2$ may have the $Cu(TCNQ^0)(TCNQ^-)$ composition. The binding energy values of these two N 1s features lie very close to those in $TCNQ^0$ and $TCNQ^-$, adding further evidence to the proposed mixed-valence type formula for this compound. As further evidence for this composition we show in Figure 4 N 1s spectra for $TCNQ^0$ and CuTCNQ and their sum, labeled "Synthesis Spectrum". The synthesis spectrum matches quite well the overall shape and structure of the N 1s spectrum for $Cu(TCNQ)_2$, also shown in Figure 4.

C 1s Region. Many of the comments made concerning the N 1s region spectra for $TCNQ^0$ and the TCNQ compounds are applicable to the C 1s region spectra in the corresponding compound. Also, as shown in Figure 5, the C 1s spectra for $Cu(TCNQ)_2$ can be synthesized from addition of spectra from $TCNQ^0$ and CuTCNQ.

We now shift our discussion to the specifics of C 1s peak shapes of the charge-transfer compounds with respect to $TCNQ^0$. Although the general structures of the C 1s peaks are similar they are not identical. We can make use of these differences to discuss slight variations in charge transfer in each compound.

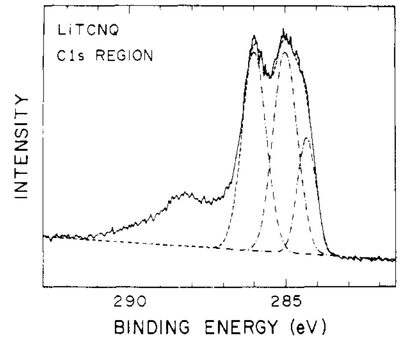

Figure 6. High-resolution C 1s X-ray photoelectron spectrum for LiTCNQ. Solid line indicates experimental data. Dash–dot lines indicates the three components to the fitting procedure described in the text. Dashed curve is the sum of the three components.

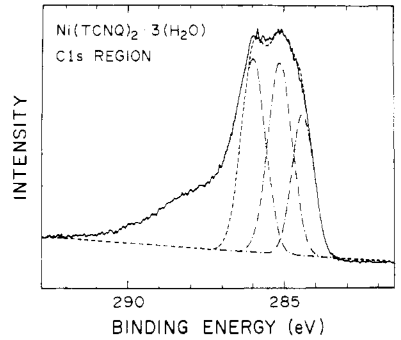

Figure 7. High-resolution C 1s X-ray photoelectron spectrum for $Ni(TCNQ)_2{\cdot}3H_2O$. Solid line indicates experimental data. Dash–dot lines indicate the three components to the fitting procedure described in the text. Dashed curve is the sum of the three components.

As presented in Table I, the binding energies of the two C 1s features of $TCNQ^0$ shift on compound formation ca. 0.6 and 0.3 eV to lower values for the high- and low-binding-energy features respectively. The high-binding-energy feature has been associated with emission from the methylene and cyano type carbons in $TCNQ^0$. The low-binding-energy feature stems from emission from the ring carbons.[12] Thus, neglecting final-state effects, these binding-energy shifts on compound formation indicate a relatively large amount of e^- density is redistributed from the metal donor atom to carbon atoms outside the six-membered ring of TCNQ, resulting in the larger shift for the high-binding-energy peak. This localization of transferred electron density away from the ring correlates well with conclusions of our previous work, which localizes the lowest unoccupied molecular orbital of $TCNQ^0$ (the orbital involved in charge transfer) in this region of the molecule.[12] This is also in agreement with high-resolution electron micrographs of TCNQ–metal charge-transfer compounds which locate metal atoms bonded adjacent to TCNQ cyano groups in the compound.[14]

A close examination of the main C 1s features in spectra of these compounds reveal some subtle differences in peak shapes. In each of these spectra there seems to be a shoulder at the *low-binding-energy* side of the C 1s spectra. This is most obvious in comparison with $TCNQ^0$ in Figure 2. In Figures 6–8, the lower binding energy region (the

---

(14) Uyeda, N.; Kobayashi, T.; Ishizuki, K.; Fujiyoshi, Y.; Inokuchi, H.; Saito, G. *Mol. Cryst. Liq. Cryst.* **1985**, *125*, 103.

(15) Larsson, S. *Chem. Phys. Lett.* **1976**, *40*, 362.

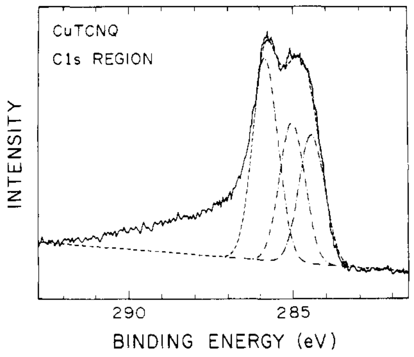

Figure 8. High-resolution C 1s X-ray photoelectron spectrum for CuTCNQ. Solid line indicates experimental data. Dash–dot lines indicate the three components to the fitting procedure described in the text. Dashed curve is the sum of the three components.

nonshakeup region) of the spectra have been fit to three 100% Gaussian shaped peaks. The peak fitting procedure involved, first matching the low-binding-energy side of the spectrum with a single peak, then the high-binding-energy side of the spectrum, and then adding a third peak between the two to give the sum of the three peaks that best overlap with the spectrum, ignoring the tail to high binding energy. While this peak-fitting procedure is strictly qualitative, it seems clear that more than two chemically distinct carbon atoms can be identified in the charge-transfer compounds. This is in striking contrast to the $TCNQ^0$ spectra, which clearly show only two peaks. The fact that we can separate only two carbon peaks from $TCNQ^0$ while there exist four theoretically distinct carbon environments has been discussed in detail previously.[12]

The lowest binding-energy feature in each synthesized spectrum for the charge-transfer complexes lies at ~284.3 eV. The large difference in binding energy of this feature from the two C 1s peaks of $TCNQ^0$ indicates the carbon moiety undergoing emission is most likely in a new chemical environment in $TCNQ^-$. It is possible this peak stems from emission of carbons most directly interacting with the metal donor and thus receiving the most charge donation. The carbon peaks at ~286.0 and ~285.1 eV are assumed to be shifted features from the $TCNQ^0$ spectrum. From the bonding configuration of the metal and $TCNQ^-$ ion in the compound it is logical to propose the new carbon moiety is at or near the ends of the molecule, i.e., outside the ring. Remembering that carbon atoms outside the ring give rise to emission at 286.6 eV in $TCNQ^0$, this would correspond to a binding energy shift of 2.3 eV. Electronic structure calculations of Jonkman et al.[7] indicate that the largest change in atomic charge on formation of $TCNQ^-$ occurs for the two methylene-like carbons, in agreement with the arguments outlined above.

Metal Core Level Regions. The Li and Cu core level spectra of the charge-transfer compounds described here are consistent with a +1 oxidation state of these metal atoms, while the Ni spectra are consistent with a +2 oxidation state. In particular, as shown in Table III the Ni $2p_{3/2}$ binding energy in $Ni(TCNQ)_2{\cdot}3H_2O$ is shifted by ~4.7 eV to higher binding energy compared with Ni metal and the Li 1s binding energy in LiTCNQ is the same as observed for LiF. The Cu core level spectra for CuTCNQ and $Cu(TCNQ)_2$ actually show small shifts to *lower* binding energy compared to Cu metal. However, the core binding energies for Cu are well-known to be affected by large final-state relaxation effects and thus are not good indicators of the Cu oxidation state. For example, the $2p_{3/2}$ binding energy for Cu in CuCN is within 0.2 eV of that for Cu metal. The auger parameter, however, has been more useful as a monitor of the Cu oxidation state. The Auger parameter for Cu in CuCN (see Table II) is 1847.5, shifted by 3.7 eV from the value of 1851.2 that we observe for metallic Cu. The Auger parameters of 1847.9 and 1847.6 that we observe for CuTCNQ and $Cu(TCNQ)_2$ are thus very consistent with an assignment of +1 oxidation state for the Cu in these compounds. In addition, if the Cu were in the +2 oxidation state in $Cu(TCNQ)_2$, one would expect substantial satellite structure in the 2p region of the spectrum, which we do not observe.

Satellite Structure and Conductivity. In addition to the shift to lower binding energy of the main N 1s feature and the change in the main C 1s peaks for the charge-transfer compounds compared to $TCNQ^0$, there are significant differences in the shape of the high-binding-energy side of the peaks. In the $TCNQ^0$ spectra a well-resolved shakeup satellite is observed at a binding energy 2.6 eV above both the N 1s and C 1s peaks. The shakeup satellite originates from a core photoionization event which also leaves the resulting ion in an excited valence state. A detailed discussion of this satellite has been published previously for the case of $TCNQ^0$.[12] The spectra of the charge-transfer compounds exhibit less well-resolved satellites. The LiTCNQ and $Ni(TCNQ)_2{\cdot}3H_2O$ spectra have weak satellites centered at ~2.6 eV greater binding energy than the main peak with a continuous background intensity that merges into the high-binding-energy side of the main N 1s and C 1s peaks. The structure at 2.6 eV is presumed to result from a final-state excitation similar in nature to that observed for $TCNQ^0$. In analogy the development of a continuous background would correspond to a continuous distribution of final-state excitations. The case of $Cu(TCNQ)_2$ is complicated by the overlapping of the spectra from the $TCNQ^-$ and $TCNQ^0$ components. If one looks at the sequence LiTCNQ, $Ni(TCNQ)_2{\cdot}3H_2O$, and Cu(TCNQ), a trend is observed in the shape of the high-binding-energy tails. The Li(TCNQ) spectra exhibit a substantial peak shifted by 2.6 eV with a slight intensity in the valley between the satellites and the corresponding main N 1s and C 1s peaks. The $Ni(TCNQ)_2{\cdot}3H_2O$ spectra exhibit a noticeable but substantially less well defined satellite shifted by 2.6 eV from the N 1s and C 1s main features and increased intensity closer to the main peaks. In the CuTCNQ spectra little is left of the peak in intensity at a shift of 2.6 eV. An essentially continuous tail to higher binding energy is observed for the C 1s spectra, while a shoulder with substantial continuous background is observed shifted by only 1.2 eV from the main N 1s peak. Thus the trend observed in going from Li(TCNQ) to $Ni(TCNQ)_2{\cdot}3H_2O$ to Cu(TCNQ) is toward a more continuous high-binding-energy tail to the N 1s and C 1s peaks. Also, this high-binding-energy tail moves in closer to the main peaks in this sequence. The sequence LiTCNQ, $Ni(TCNQ)_2{\cdot}3H_2O$, Cu(TCNQ) also corresponds to increasing conductivity in these compounds, as indicated in Table III. The data shown in Table III were obtained by using pressed pellets. While there can be substantial problems in the use of such samples for absolute conductivity measurements, these values should provide a reasonable comparison between the compounds in this study. In particular we are interested in the fact that the conductivity of the Li compound is substantially lower than the others and the two copper compounds are quite similar. The data shown in Table III are for room-temperature samples. While the absolute values of the conductivities have been shown to be temperature dependent, the trend of conductivities in these compounds does not change with temperature.

As mentioned previously, the electrical conductivity of TCNQ charge-transfer complexes has been of interest for some time. The compounds of interest in this study have conductivities in the range typical for semiconductors. The conductivity of TCNQ charge-transfer complexes is believed to be associated with the degree of electron transfer from the donor to the TCNQ. As discussed by Torrance,[8] one suggested mechanism for the conductivity in TCNQ complexes involves a mixed-valence compound with two distinct TCNQ species of different oxidation state in the structure, $TCNQ^0$, and $TCNQ^-$. Delocalization over these distinctly different species then is proposed to lead to high conductivity. $Cu(TCNQ)_2$ is such a compound, with both $TCNQ^0$ and $TCNQ^-$ species in the structure. However, the conductivities of $Cu(TCNQ)_2$ and CuTCNQ (which has only $TCNQ^-$ in the structure) are essentially identical. Thus at least in this case the existence of two oxidation states of TCNQ in the $Cu(TCNQ)_2$ structure does not appear to have any effect on the conductivity.

The correlation of the shape of the intensity on the high-binding-energy side of the core level peaks with the conductivity of the compounds is what one would expect if the valence state involved in the satellite observed for $TCNQ^0$ is the one that eventually leads to conductivity. Essentially what we are observing is the development of a continuous band from an intially localized excited state.

Summary

The X-ray photoelectron spectra presented here for the charge-transfer complexes of TCNQ have provided several insights into the bonding and properties of these compounds. The points we would like to stress are as follows:

The TCNQ moiety in LiTCNQ, $Ni(TCNQ)_2 \cdot 3H_2O$, and CuTCNQ exists as the $TCNQ^-$ species.

The oxidation state of Cu is +1 in both CuTCNQ and $Cu(TCNQ)_2$.

The $Cu(TCNQ)_2$ compound consists of one $TCNQ^-$ species and one $TCNQ^0$ species. Since the conductivities of CuTCNQ and $Cu(TCNQ)_2$ are essentially identical, the importance of a mixed-valence mechanism for conductivity is questionable for these compounds.

The C 1s spectra of the charge-transfer compounds are consistent with a more complex chemical environment than in $TCNQ^0$ and can be described by the assumption that the carbon atoms that interact most directly with the electron donor give rise to a low-binding-energy shoulder of the C 1s spectra. The fitted spectra indicate a 2.3-eV binding energy shift between the extra-ring carbons in $TCNQ^0$ and this most strongly interacting carbon.

The evolution of the localized shakeup peak observed in the N 1s and C 1s spectra of TCNQ into a continuous high-binding-energy tail for CuTCNQ is consistent with the development of a band that involves the excited valence orbital responsible for the shakeup feature. This is consistent with our previous assignment of the $TCNQ^0$ shakeup feature to a final-state excitaion involving the lowest unoccupied molecular orbital of TCNQ.

As was pointed out in the Introduction, the spectra presented here will also provide comparisons that should help greatly in the understanding of the chemistry of few-layer-thick films of TCNQ on the transition metals Cu and Ni. Experiments on such thin films are under way in our laboratory.

Acknowledgment. This work was supported in part by the Office of Naval Research. J.C.H. thanks the Alfred P. Sloan Foundation for fellowship support. J.M.L. thanks IBM for support as an IBM Graduate Research Fellow.

Uniform Colloidal Zinc Compounds of Various Morphologies

Maurizio Castellano[†] and Egon Matijević*

Department of Chemistry, Clarkson University, Potsdam, New York 13676

Received July 29, 1988

The preparation of finely dispersed zinc compounds consisting of uniform particles is described. Aging at elevated temperatures (~90 °C) of aqueous solutions of zinc nitrate or zinc chloride in the presence of urea resulted in precipitation of uniform rodlike basic zinc carbonate particles. These solids show X-ray characteristics of crystalline hydrozincite. In the presence of sulfate ions amorphous spherical particles of narrow size distribution of the same chemical composition are generated. On calcination both kinds of solids change to zinc oxide yet retain the original shape. In the presence of NaH_2PO_4 and urea, aqueous zinc salt solutions on aging yield rather uniform amorphous spherical zinc basic phosphate particles, which on calcination lose water.

Introduction

Solid zinc compounds are used in numerous applications. For example, zinc hydroxide carbonate, naturally occurring as hydrozincite, is of interest as such but also as a precursor to zinc oxide.[1-3] Catalytic activities of zinc carbonate in hydrogenation of oils,[4] in polymerization of cyclic ethers, and in synthesis of acetonitrile[5] have been reported. These materials have been used as fillers in rubber manufacture, pigments, storage batteries, etc. They are also common products of corrosion of zinc in moist air.

Zinc oxide has been employed traditionally in rubber and paint industries, for coatings, in ceramics, and in production of varistors. It is an intrinsic semiconductor[6] and exhibits high piezoelectricity.[7]

[†] On leave from Eniricerche, Milano, Italy.

(1) Krause, A.; Plura, I. *Monatsh. Chem.* **1965**, *96*, 1581.
(2) Utsugi, H.; Tamiya, K. *Nippon Kagaku Zasshi* **1965**, *86*, 699.
(3) Shekhter, A. B.; Moshkovskii, S. H. *Dokl. Akad. Nauk SSSR* **1950**, *72*, 339.
(4) Teruyama, K.; Kobashi, A.; Nobori, H. *J. Chem. Soc. Jpn., Ind. Chem. Sect.* **1951**, *54*, 401.
(5) Ishiguro, T.; Kitamura, E.; Kubota, S.; Tabata, N. *J. Pharm. Soc. Jpn.* **1962**, *72*, 607.
(6) Greenwood, N. N. *Ionic Crystals, Lattice Defects and Nonstoichiometry*; Butterworths: London, 1969.

0897-4756/89/2801-0078$01.50/0 © 1989 American Chemical Society